The Magnetic Structure of $GdAgSb_2$ Determined by X-ray Resonant Exchange Scattering

C. Song, W. Good, D. Wermeille, J. Kim,
A. I. Goldman, S. Bud'ko, P. C. Canfield
Ames National Laboratory and Department of Physics and Astronomy, Iowa State University, Ames, IA, U.S.A.

Introduction

The recent availability of high-quality single-crystal samples of $RAgSb_2$ (R = rare earth ion) compounds has stimulated new interest in the highly anisotropic electronic and magnetic properties of these materials and their manifestation in various physical phenomena [1, 2].

Most of the $RAgSb_2$ compounds display long-range antiferromagnetic ordering at low temperature [3]. The reported transition temperatures for the heavy rare earth compounds scale with the de Gennes factor, indicating that the Ruderman-Kittel-Kasuya-Yoshida (RKKY) interaction is the primary exchange interaction between local moments of the rare earth ions [1, 3]. For the light rare earth compounds, however, there are significant deviations from de Gennes scaling that are claimed to result from the influence of strong crystalline electric field (CEF) effects [3].

Because of the fact that the orbital angular momentum L for the *4f*-orbitals of Gd equals zero, $GdAgSb_2$ should be free of CEF effects, a determination of the magnetic structure of this system can help to resolve issues regarding the role of CEF effects on magnetic ordering in this family of compounds. The extensive neutron scattering experiments on powder samples of $RAgSb_2$ compounds reported by André et al. [4], however, did not include the Gd-compound, presumably because of the neutron opacity of the naturally abundant Gd ion.

Methods and Materials

Single crystals of $GdAgSb_2$ were grown by using a high-temperature flux technique at Ames Laboratory [5]. The resulting crystals are shaped as platelets, with the flat surface perpendicular to the crystallographic ***c*** direction (the [00*l*] unique axis of the tetragonal structure). Further polishing of the sample surface was not possible without degrading the sample quality (increasing the sample mosaicity) because of its softness. For the magnetic x-ray diffraction experiment, the cleanest sample, without noticeable flux inclusions from the growth process, was chosen. For this sample, the mosaic was measured to be 0.015° at the (008) reflection at 17 keV.

The resonant x-ray scattering experiments were carried out on in the Midwest Universities Collaborative Access Team (MU-CAT) 6-ID undulator beamline at sector 6 of the APS by using a double-crystal Si(111) monochromator. Polarization analysis of the scattered radiation was accomplished by using a pyrolytic graphite (PG) (006) analyzer set to scatter in the horizontal plane (perpendicular to the sample scattering plane). In this configuration, the analyzer scattering angle is close to 90° at the Gd L_3 absorption edge, and the σ-polarized component (polarization vector out of the sample scattering plane) of the scattered radiation is effectively suppressed by the analyzer. By moving from the PG (006) reflection to the PG (002) reflection, the analyzer scattering angle changes from 99.6° to 29.5°, allowing the σ-polarized component to pass as well.

The single crystal of $GdAgSb_2$ was mounted on a copper rod attached to the cold finger of a closed-cycle cryogenic refrigerator. The sample was oriented with the (*h*0*l*) zone in the scattering plane. The polarization of the incident beam (predominantly σ-polarized) was perpendicular to the scattering plane; i.e., parallel to the [0*k*0] direction for any (*h*0*l*) reflections.

Results

At low temperature, in the purely π-polarized channel, a resonant scattering signal was observed at positions corresponding to a magnetic wave vector of $\tau = (0½0)$, whereas no signal was observed on the $\tau = (½00)$ positions. However, after changing the scattering angle of the analyzer crystal to make use of the PG (002) reflection, allowing both σ and π scattering to pass, magnetic peaks were observed at positions corresponding to $\tau = (½00)$. These results indicate that the ordered moment direction in the antiferromagnetic state is oriented perpendicular to the magnetic wave vector. The energy profiles depicted in Figure 1 show both the dipolar origin of the scattering at the (0-½8) reflection, arising from the strong interaction between the core hole in the $2p_{3/2}$ orbital and the 5*d* band, and the quadrupolar origin of the scattering at the (½08) reflection, arising from the weaker interaction between the $2p_{3/2}$ core hole and the strongly localized 4*f* band [6, 7].

To confirm that the resonant enhancement at the (½08) magnetic peak arises from electric quadrupole transitions with the moment transverse to the magnetic wave vector, Q-dependent integrated intensity measurements were performed by using those magnetic peaks (½0*l*) that could

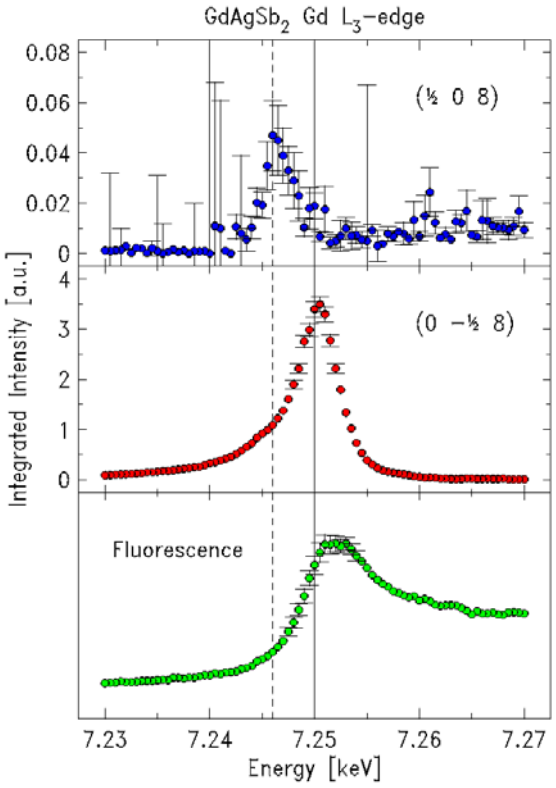

FIG. 1. Integrated intensity of the (½08) (upper panel) and (0-½8) (middle panel) reflections of $GdAgSb_2$ as a function of energy across the Gd L_3 edge in the low-temperature magnetic phase. The background fluorescence from the sample is shown in the lower panel.

be accessed in the symmetric scattering geometry. The integrated intensity was measured with open detector slits by using the PG(002) reflection from the analyzer crystal. The rather broad mosaic of the analyzer, ~0.5°, is significantly larger than the full width at half maximum (FWHM) of magnetic satellites of ~0.1°, ensuring adequate integration of the scattered intensity. Proper integration over 2θ and χ was achieved by opening the detector slits until a flat top was observed in 2θ and χ scans through the magnetic peaks. The integrated intensities of several peaks that could be accessed in this geometry were calculated from rocking scans of the sample crystal through the magnetic reflections. The observed integrated intensities of the magnetic satellite are plotted in Fig. 2. The solid line represents a fit to the theoretical quadrupole resonance scattering cross section with the moment direction along [010], showing reasonable agreement with the data.

The temperature dependence of the integrated intensity ($I = \sim\mu^2$) of the (½08) magnetic satellite peak at the L_3 resonance energy is displayed in Fig. 3. The solid line is a

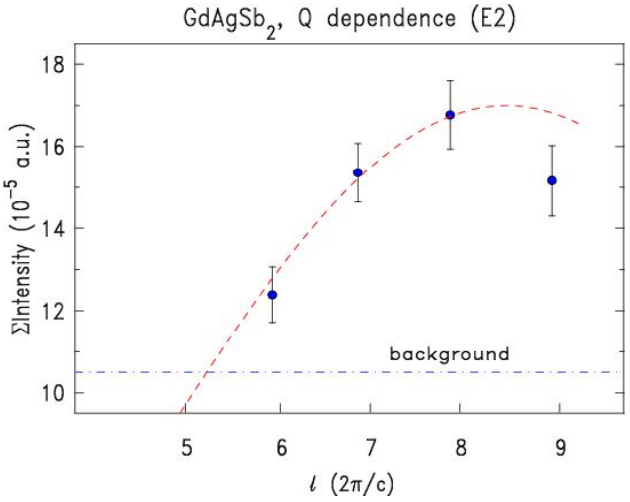

FIG. 2. Q-dependent integrated intensity of (½0l) magnetic satellites of $GdAgSb_2$ at 8K. The dashed line is the calculated E2 cross section for a magnetic moment direction along [010].

fit to the power law, $I = \sim A(T_N - T)^{\beta}$. A transition temperature $T_N = 13.0$K obtained from the fit is close to the value $T_N = 12.8$K obtained from the bulk susceptibility measurement [1].

Discussion

The principal result of this work is the *ab initio* determination of the magnetic structure of $GdAgSb_2$ by x-ray resonance exchange scattering. Below 13K, the local magnetic moments order antiferromagnetically, doubling the unit cell along the ***a*** direction (or equivalently in the tetragonal structure ***b*** direction) in the basal plane, with the moments ordered transverse to this direction also being within the basal plane. These results indicate that the commensurate antiferromagnetic ordering observed in several of the $RAgSb_2$ compounds is not necessarily driven by the strong CEF effects as proposed by André et al. Indeed, it should be noted that in the related RNi_2B_2C family, the Gd compound, as well as many of the strongly anisotropic member compounds (R = Er, Tb, Ho), order in an incommensurate structure determined largely by Fermi surface nesting [8, 9].

The interactions that conspire to produce magnetic ordering in many of these systems are quite complex, involving RKKY-type indirect exchange, CEF anisotropies, and, especially for the light rare earths, hybridization effects and possible changes in the indirect exchange coupling. A great deal of further study is clearly necessary to unravel the contributions of all of these mechanisms.

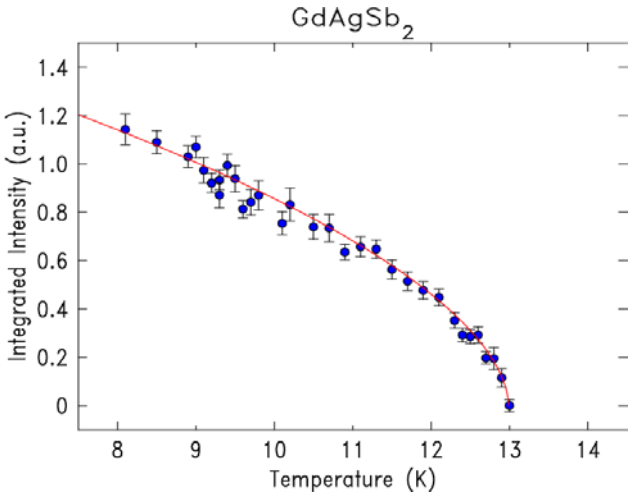

FIG. 3. Temperature dependence of the integrated intensity of the (½08) magnetic satellite of $GdAgSb_2$. The solid line is a fit to a power law as described in the text.

Acknowledgments

Ames Laboratory (U.S. Department of Energy [DOE]) is operated by Iowa State University under Contract No. W-7405-ENG-82. Synchrotron work was performed at the MU-CAT sector at the APS. Use of the APS was supported by the DOE Office of Science, Office of Basic Energy Sciences, under Contract No. W-31-109-ENG-38.

References

[1] K. D. Meyers, S. L. Bud'ko, I. R. Fisher, Z. Islam, H. Kleinke, A. H. Lacerda, and P. C. Canfield, J. Magn. Magn. Mater. **205**, 27 (1999).
[2] K. D. Meyers, S. L. Bud'ko, V. Antropov, B. N. Harmon, and P. C. Canfield, Phys. Rev. B **60**, 13371 (1999).
[3] G. André, F. Bourée, M. Kolenda, B. Lesniewska, A. Oles, and A. Szytula, Physica B **292**, 176 (2000).
[4] G. E. Bacon, *Neutron Diffraction*, 3rd edition (Oxford, 1975), p. 73.
[5] P. C. Canfield and Z. Fisk, Philos. Mag. B **56**, 7843 (1992).
[6] P. Carra, B. N. Harmon, B. T. Thole, M. Altarelli, and G. A. Sawatzky, Phys. Rev. Lett. **66**, 2495 (1991).
[7] X. Wang, T. C. Leung, B. N. Harmon, and P. Carra, Phys. Rev. B **47**, 9087 (1993).
[8] J. W. Lynn, S. Skanthakumar, Q. Huang, S. K. Sinha, Z. Hossain, L. C. Gupta, R. Nagarajan, and C. Godart, Phys. Rev. B **55**, 6584 (1997).
[9] C. Stassis and A. I. Goldman, J. Alloys Compd. **250**, 603 (1997).